Building-Block Diversity in Polydopamine Underpins a Multifunctional Eumelanin-Type Platform Tunable Through a Quinone Control Point

*Nicola F. Della Vecchia, Roberto Avolio, Michela Alfè, Maria E. Errico, Alessandra Napolitano, and Marco d'Ischia**

Rational approaches to engineering polydopamine films with tailored properties for surface coating and functionalization are currently challenged by the lack of detailed information about the polymer structure and the mechanism of buildup. Using an integrated chemical and spectroscopic approach enables the demonstration of: a) a three-component structure of polydopamine, comprising uncyclized (catecholamine) and cyclized (indole) units, as well as novel pyrrolecarboxylic acid moieties; b) remarkable variations in the relative proportions of the cyclized and uncyclized units with starting dopamine concentration; c) the occurrence of oligomer components up to the tetramer level; d) the covalent incorporation of Tris buffer; and e) the role of dopamine quinone as a crucial control point for directing the buildup pathways and tuning the properties. The importance of the uncyclized amine-containing units in polydopamine adhesion is also highlighted. The proper selection of substrate concentration and buffer is thus proposed as a practical means of tailoring polydopamine functionality via control of competing pathways downstream of dopamine quinone.

1. Introduction

Catecholamine compounds, such as L-3,4-dihydroxyphenylalanine (L-dopa) and the neurotransmitters dopamine and norepinephrine, are prone to oxidation to *o*-quinones, leading eventually to black insoluble biopolymers, commonly referred to as melanins or, more properly, "eumelanins", implicated in human pigmentation, melanoma genesis, and neuromelanin synthesis in the brain.[1–8] In 2007 it was demonstrated that suitable mimicking of these bioprocesses could provide an access route to highly resistant and adhesive materials suitable for the deposition of films and multifunctional coatings.[9] Accordingly, over the past few years, the black oxidation product of dopamine, commonly referred to as polydopamine or dopamine-melanin, has burst onto the scene of materials science as a versatile biomaterial for broadly diverse applications.[10–18] Currently, the scope of polydopamine research is rapidly expanding to include energy applications (e.g., batteries,[19] microfluidic systems,[20] and water-condensing devices).[21] A remarkable intrinsic property of polydopamine films is the reversible and pH-switchable permselectivity for both cationic and anionic redox-active probe molecules, suggesting application in ion gate-based technology.[22]

So far, insights into the fundamental building blocks of polydopamine and their covalent and/or supramolecular organization have been thwarted by the marked chemical heterogeneity and adverse physical properties of this material. However, as applications of polydopamine become ever more sophisticated and technologically demanding, there appears to be an increasing need to define the basic structure-property-function relationships and to devise rational chemical strategies directed at optimizing and/or tailoring functionality.

Until 2012, application-oriented researchers had assumed either of two opposed and speculative structural models: the "open-chain polycatechol/quinone" model, envisaging linear sequences of catecholamine units linked through biphenyl-type bonds, and the "eumelanin" model, which envisages a polymeric skeleton based on the key cyclization product of dopamine, namely 5,6-dihydroxyindole (DHI)[9,23–25] (**Scheme 1**). However, neither of these models was founded on solid experimental evidence, nor were they related to specific polydopamine properties and functions.

When this manuscript was almost complete, two independent papers appeared, in which the nature of polydopamine was re-examined. In one paper,[26] data from

Dr. N. F. Della Vecchia, Prof. A. Napolitano, Prof. M. d'Ischia
Department of Chemical Sciences
University of Naples Federico II
Via Cintia 4, I-80126 Naples, Italy
E-mail: dischia@unina.it
Dr. R. Avolio, Dr. M. E. Errico
Institute of Chemistry and Technology of Polymers
National Council of Research (CNR)
via Campi Flegrei 34, Pozzuoli I- 80078, Italy
Dr. M. Alfé
Combustion Research Institute
National Council of Research (CNR)
Piazzale V. Tecchio 80, I–80125 Naples, Italy

DOI: 10.1002/adfm.201202127

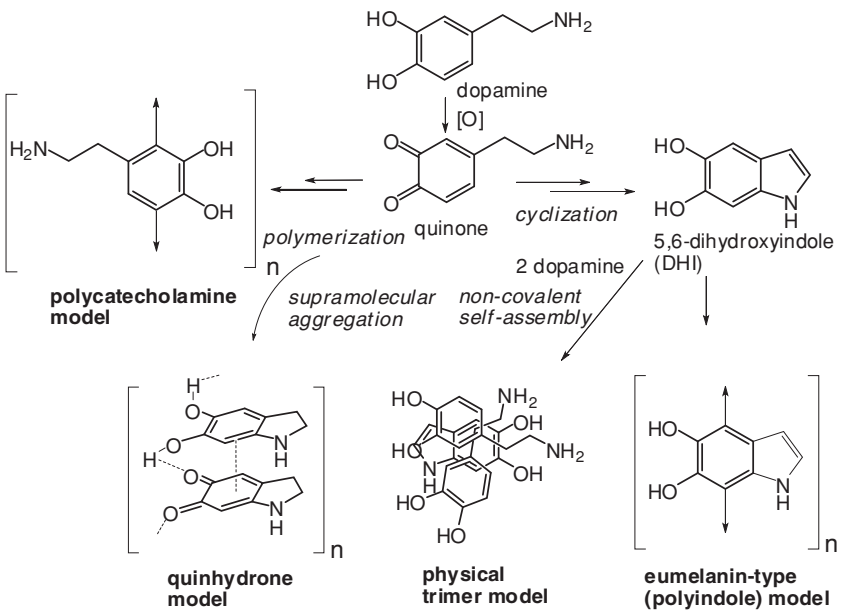

Scheme 1. Traditional and recent models of the polydopamine structure.

solid-state spectroscopic and crystallographic techniques suggested that polydopamine is not a covalent polymer, as generally agreed, but is rather a supramolecular aggregate of monomers (consisting primarily of 5,6-dihydroxyindoline and its dione derivative, dopaminochrome), which are held together through a combination of charge transfer, π-stacking, and hydrogen-bonding interactions. In the other study,[27] high-performance liquid chromatography (HPLC) analysis coupled with mass spectrometry allowed the identification of a physical trimer of (dopamine)2/DHI, derived from a self-assembly mechanism leading to a significant non-covalent component of polydopamine (Scheme 1).

Capitalizing on our previous experience in the field of eumelanin biopolymers and 5,6-dihydroxyindole chemistry,[28–34] we have recently been prompted to undertake a systematic investigation aimed at filling major gaps in the understanding of the polydopamine structure, at integrating and expanding currently emerging models, and at setting out a reliable working framework that may allow for direct control of functionality. The specific goals of this study were: 1) to elucidate the nature of the basic structural units and their relative proportions in polydopamine preparations obtained under reported conditions of technological relevance; 2) to determine the degree of polymerization in the main components; c) to assess and rationalize the influence of the varying experimental parameters in the synthetic protocols for polydopamine coating or film deposition on the structural characteristics of the final polymer.

2. Results and Discussion

2.1. Polydopamine Analysis by Chemical Degradation

Different sets of polydopamine samples were prepared at two dopamine concentrations (0.5×10^{-3} and 10×10^{-3} M) and in three different reaction media, namely 0.1 M bicarbonate, 0.05 M Tris buffer, and 0.1 M phosphate buffer, with the pH kept constant in all of the experiments at 8.5. All of the reactions were run in air under stirring with a similar supply of oxygen, and were halted after 24 h. The only exception was the reaction of 0.5×10^{-3} M dopamine in Tris buffer at pH 8.5, which did not produce a collectable precipitate until 72 h of autoxidation. The yields of the pigments obtained under the different reaction conditions explored are reported in Table S1 in the Supporting Information. The fundamental structural units and their modifications were determined by an integrated approach based on chemical degradation followed by eumelanin-marker determination and solid-state-NMR investigations.

Due to their heterogeneity and insolubility in all solvents, eumelanin-type pigments are usually characterized by oxidative degradation (e.g., with alkaline hydrogen peroxide), followed by HPLC quantitation of two diagnostic degradation markers, pyrrole-2,3-dicarboxylic acid (PDCA) and pyrrole-2,3,5-tricarboxylic acid (PTCA).[35–37]

PDCA and PTCA are formed in very low yields (<2% on a weight basis) by the oxidative breakdown of indolequinone moieties of eumelanins, giving also exceedingly complex mixtures of carboxyl-containing fragments of limited structural significance (e.g., oxalic acid).[1] Nonetheless, both pyrroles are generally recognized as being highly specific and reliable markers of eumelanin-type polymers, and their quantitative determination provides the basis of established microanalytical methodologies in biological samples and tissues.[36]

PTCA derives from 2-linked DHI units, either inner or terminal, whereas PDCA would derive primarily from terminal indole units unsubstituted at the 2-position, based on the known mode of polymerization of DHI via 2,4′- and 2,7′-bonding patterns.[29] As apparent from the simplified oligomer/polymer chain model (Supporting Information, Scheme S1), the contribution of inner units to PDCA is expected to be negligible since it is unlikely to find 2-unsubstituted inner units within DHI oligomers.[29] Although it is also possible to envisage non-terminal PDCA-yielding units at branching points of oligomeric structures, reflecting phenyl-ring coupling of dopamine, branching mechanisms in phenol/catechol coupling processes have so far been little documented. It seemed therefore convenient for the purposes of this study to keep Scheme S1 in the Supporting Information as a reasonable structural framework for the interpretation of the data.

On this basis, a quantitative determination of PTCA and PDCA was used to assess: a) the relative proportion of DHI-derived units in polydopamine, using pure DHI eumelanin as a reference; and b) the number of 2-linked versus terminal 4- or 7-linked units. It is reasonable to assume, with this aim, that PDCA-yielding units occupy mainly terminal positions and that the PTCA/PDCA ratio, reflecting the inner-to-terminal unit ratio, is roughly proportional to the degree of polymerization.

Table 1. Yields of PTCA and PDCA produced by oxidative degradation of polydopamine samples.

Sample #	Substrate Concentration [$\times 10^{-3}$ M]	Oxidant/buffer (pH 8.5)/reaction time	Yield[a] [% w/w]			
			PDCA	PTCA	PTCA + PDCA	PTCA/PDCA
1	Dopamine 0.5	O_2/0.1 M $NaHCO_3$/24 h	1.17 ± 0.12	0.79 ± 0.08	1.96 ± 0.20	0.67
2	Dopamine 10	O_2/0.1 M $NaHCO_3$/24 h	0.76 ± 0.07	0.37 ± 0.04	1.13 ± 0.11	0.49
3	Dopamine 0.5	O_2/0.1 M phosphate/24 h	0.89 ± 0.09	0.88 ± 0.09	1.77 ± 0.18	1.00
4	Dopamine 10	O_2/0.1 M phosphate/24 h	0.79 ± 0.08	0.51 ± 0.04	1.30 ± 0.12	0.64
5	Dopamine 0.5	O_2/0.05 M Tris/72 h	0.43 ± 0.03	0.40 ± 0.03	0.83 ± 0.06	0.93
6	Dopamine 10	O_2/0.05 M Tris/24 h	0.92 ± 0.10	0.49 ± 0.04	1.41 ± 0.14	0.53
7	DHI 0.5	O_2/0.1 M $NaHCO_3$/24 h	0.81 ± 0.08	0.89 ± 0.08	1.70 ± 0.16	1.10
8	DHI 10	O_2/0.1 M $NaHCO_3$/24 h	1.21 ± 0.12	0.31 ± 0.04	1.52 ± 0.16	0.26
9	Dopamine	–	0.15 + 0.01	0.08 + 0.00	0.38 + 0.02	0.53

[a] Mean ± SD, $n = 3$.

Table 1 shows PTCA and PDCA formation yields from the chemical degradation of the six polydopamine samples mentioned above. As a control, PTCA/PDCA yields from the degradation of the starting dopamine were determined and are reported in Table 1 to allow for an estimate of the possible contribution of artifactual oxidative cyclization and polymerization occurring under the alkaline degradation conditions. In addition, two more eumelanin samples were prepared as a reference by aerial oxidation of DHI at concentrations of 0.5×10^{-3} and 10×10^{-3} M in bicarbonate buffer, at pH 8.5, under the same conditions adopted for dopamine.

The results, viewed also against previous data relating to DHI oligomers and eumelanins prepared under different conditions,[36,37] led to the following conclusions:

1) When prepared from a 10×10^{-3} M precursor, polydopamine contains lower amounts of DHI-derived units with respect to pure DHI polymer, as evidenced by the statistically significant difference in the overall yields of the PTCA+PDCA (sample 8 versus sample 2, $p < 0.005$, or sample 8 versus sample 4, $p < 0.05$); conversely, polydopamine from a 0.5×10^{-3} M precursor looks similar to DHI polymers, as deduced, for example, from the non-significant difference in PTCA+PDCA yields for sample 3 versus sample 7, $p > 0.05$).
2) The proportion of DHI units is higher in the polydopamine samples from 0.5×10^{-3} M than in those from 10×10^{-3} M dopamine, as deduced from the statistically significant difference in the overall yields of PDCA+PTCA (sample 1 versus sample 2, and sample 3 versus sample 4, $p < 0.0001$), with the noticeable exception of sample 5 obtained from 0.5×10^{-3} M dopamine in 0.05 M Tris buffer, in which DHI unit formation was significantly inhibited.
3) The degree of polymerization of the DHI indole units, as roughly judged by the PTCA-to-PDCA ratios, was higher in the polydopamine samples produced from 0.5×10^{-3} M dopamine than those produced from 10×10^{-3} M catecholamine.

2.2. Solid-State ^{13}C and ^{15}N NMR

In separate experiments, the ^{13}C and ^{15}N solid-state NMR spectra of samples 1–6 were recorded. Comparative scrutiny of the ^{13}C cross-polarization/magic-angle-spinning (CP/MAS) spectra (**Figure 1**) against those of dopamine and DHI (Supporting Information, Figure S1) suggested both cyclized (indolic) and uncyclized (dopamine-like) elements, in line with previous literature data.[23,24]

Although deconvolution of the signals proved not to be an easy task, closer analysis revealed that the relative intensity of the aliphatic versus aromatic carbon signals varies significantly from one sample to the other in a consistent manner. In particular, the polymers obtained from 10×10^{-3} M dopamine exhibited intense aliphatic resonances around $\delta = 30$ and 40 ppm, and relatively well-resolved bands in the sp^2 region around $\delta =$ 115, 130, and 145 ppm, revealing a certain similarity with the spectrum of the parent dopamine (see Supporting Information, Figure S1a) and, hence, a substantial proportion of uncyclized units. Less-intense aliphatic carbon peaks could be observed in the spectra of the polydopamine samples from 0.5×10^{-3} M dopamine. In this latter case, the sp^2 carbon-peak profile was more complex, with relatively intense resonances around $\delta =$ 130 and 170 ppm, and less-intense peaks around $\delta = 145$ ppm. These differences indicate a higher proportion of cyclized indole units. Most interestingly, the presence of intense resonances around $\delta = 170$ ppm and the decreased peak area at $\delta =$ 145 ppm suggest high proportions of carboxylic acid groups and/or other carbonyl-type groups generated at the expenses of OH-bearing carbons via oxidative fission of catechol moieties in DHI units. Consistent with this conclusion is the presence of similar downfield peaks in the spectrum of the DHI polymer (sample 8, Supporting Information, Figure S3a). Carboxyl-type carbon signals were not detectable in the 10×10^{-3} M dopamine polymerization samples, with the sole exception of sample 2 generated in bicarbonate. This latter sample gave a spectrum

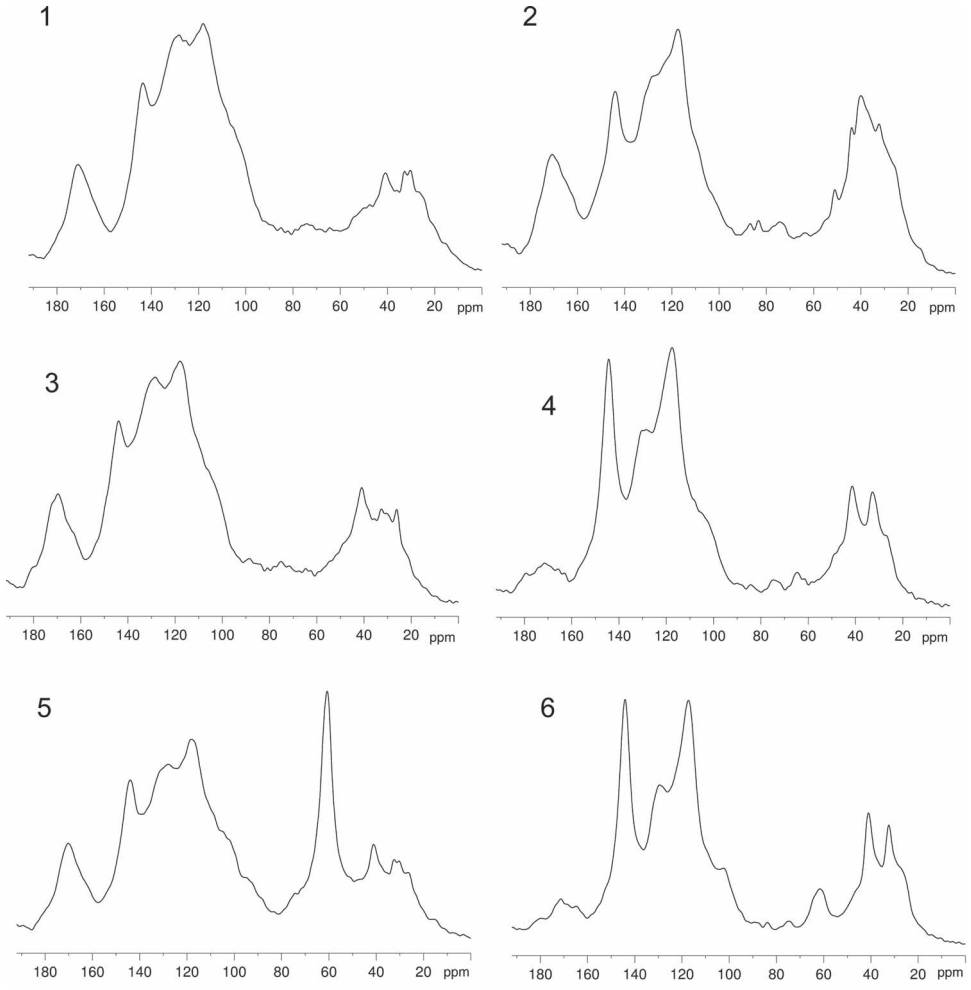

Figure 1. ^{13}C solid-state NMR spectra of the polydopamine samples. The sample labeling and oxidation conditions are as indicated in Table 1: Starting dopamine concentrations: 0.5×10^{-3} M (samples 1, 3, 5) and 10×10^{-3} M (samples 2, 4, 6). Buffer: 0.1 M bicarbonate (samples 1, 2); 0.1 M phosphate (samples 3, 4); 0.05 M Tris (samples 5, 6). The spectra were run with a contact time of 2 ms.

that was apparently different from those of the other samples from 10×10^{-3} M dopamine. It displayed a peculiar resonance profile in the aliphatic region, a broader and more-intense signal around $\delta = 130$ ppm and detectable resonances attributable to carboxylic groups. To ease the interpretation of the overlapping resonances in the sp^2 region, in representative cases ^{13}C CP/MAS spectra were recorded with shorter contact times (100 μs), enhancing C–H resonances over those from quaternary carbons. Data for samples 1 and 4 (Supporting Information, Figure S2) showed a low contribution of C–H carbons to the resonance at $\delta = 130$ ppm, suggesting a high degree of substitution of the aromatic positions.

The presence of an intense signal at $\delta = 60$ ppm in the spectrum of sample 5 obtained by autoxidation of 0.5×10^{-3} M dopamine in Tris suggests, moreover, incorporation of the buffer. This feature was apparent, though less pronounced, in the related sample 6, from 10×10^{-3} M dopamine. It could be concluded that polydopamine samples prepared in the presence of Tris may retain the buffer to a variable degree depending on the starting catecholamine concentration. Non-covalent adsorption of the buffer would be ruled out by the extensive washings to which the samples were subjected.

The ^{15}N CP/MAS spectra of samples 1–6 are reported in **Figure 2**. All of the samples obtained from the 10×10^{-3} M dopamine gave spectra exhibiting distinct nitrogen resonances in the regions typical of amine ($\delta = 30$ ppm) and indole ($\delta = 120$–140 ppm) moieties ($\delta = 125$ ppm for DHI, Supporting Information, Figure S3). Conversely, spectra from the 0.5×10^{-3} M dopamine-derived polymers were virtually devoid of high-field amine resonances, resembling those of pure DHI polymers (see for example the spectrum of sample 8 in Supporting Information, Figure S4). The only exception was sample 5, obtained from Tris buffer, which showed a broad and seemingly bifurcate peak at $\delta = 30$–40 ppm, suggesting two types of amine nitrogens as a result of the covalent incorporation of Tris into open chain dopamine units.

Most importantly, all of the polymer samples in the 0.5×10^{-3} M dopamine series displayed a broad series of peaks in the range of $\delta = 150$–170 ppm, which were less pronounced in the 10×10^{-3} M dopamine polymers obtained in phosphate and

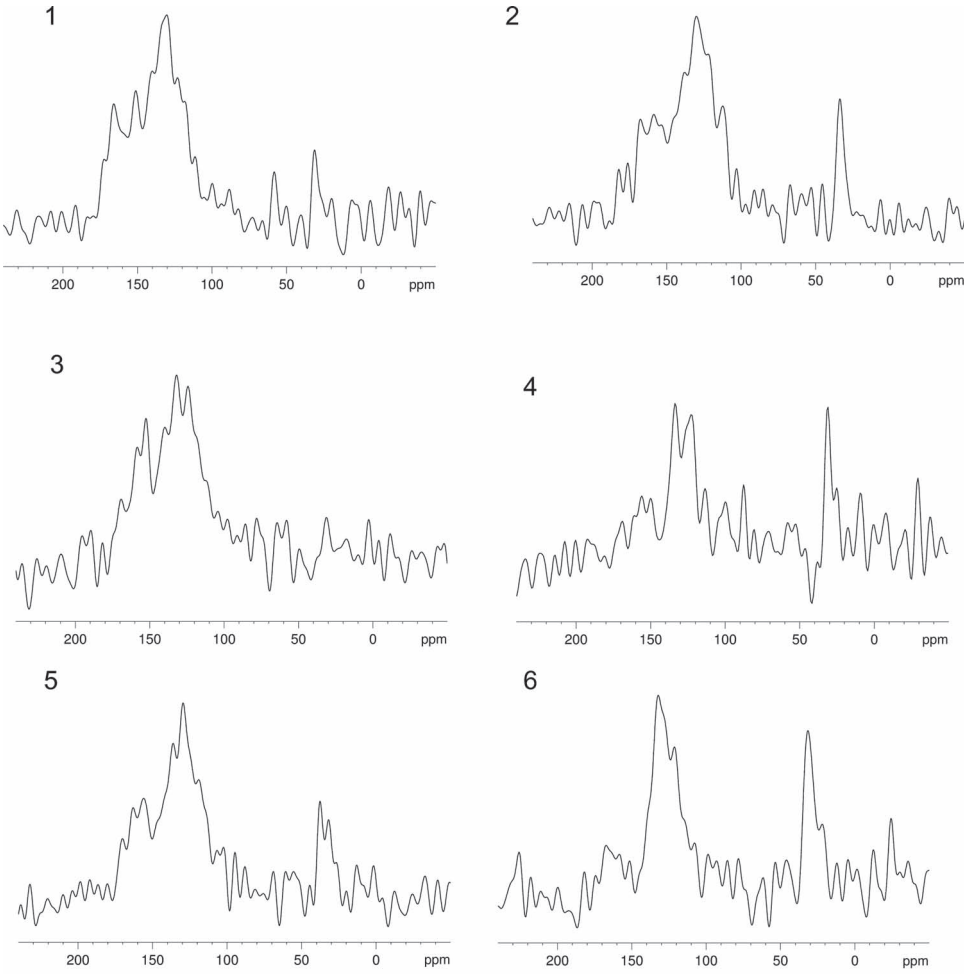

Figure 2. ^{15}N CP/MAS spectra of polydopamine samples prepared under different conditions. The sample labeling is as defined in Table 1. Starting dopamine concentrations: 0.5×10^{-3} M (samples 1, 3, 5) and 10×10^{-3} M (samples 2, 4, 6). Buffers: 0.1 M bicarbonate (samples 1, 2); 0.1 M phosphate (samples 3, 4); 0.05 M Tris (samples 5, 6).

Tris. Such resonances were downfield relative to those of DHI and typical indole derivatives[38,39] and were taken to indicate nitrogen-containing heterocyclic structures different from DHI.

Considering that: 1) the nitrogen peaks at $\delta = 150$–170 ppm are apparently accompanied by the presence of carboxyl resonances in the ^{13}C NMR spectra around $\delta = 170$ ppm, and that 2) both features are shared by the ^{15}N and ^{13}C NMR CP/MAS spectra of Sepia melanin,[38] which contains significant levels of pyrrolecarboxylic acid moieties derived from oxidative degradation of indole units,[40] it was concluded that the polydopamine samples prepared from 0.5×10^{-3} M dopamine contained both intact DHI-related units and degraded pyrrole-containing moieties as main structural components. The presence of degraded indole units provides also an explanation to the origin of the aliphatic carbon resonances ($\delta = 30$–40 ppm) in the ^{13}C spectra of the 0.5×10^{-3} M dopamine samples, which could not be assigned to ethylamine chains owing to the lack of detectable high-field amine resonances in the ^{15}N spectra. It is now proposed that such carbon resonances are due to aliphatic chains on pyrrole units generated via oxidative ring-fission processes, as reported previously.[35]

Failure to detect significant peaks at lower-field regions of the spectra (>200 ppm) suggests that Schiff base formation (e.g. via intermolecular cross-linking between a quinone ring and an amine group) would not contribute significantly to the spreading of the ^{15}N resonance of dopamine following polymerization, because of prevalent intramolecular cyclization routes leading to indole units.

Altogether, the NMR spectra provided structural information that was fairly consistent with the chemical-degradation results, with two noticeable additions:

1) Tris buffer is incorporated into the polydopamine structure, especially during oxidation of the catecholamine at relatively low concentrations.
2) DHI-related units include a proportional level of degradation products in the form of pyrrolecarboxylic acid fragments.[35]

2.3. LDI-MS Analysis

The above data supports a structural model of polydopamine in which several types of units are linked via covalent bonds to

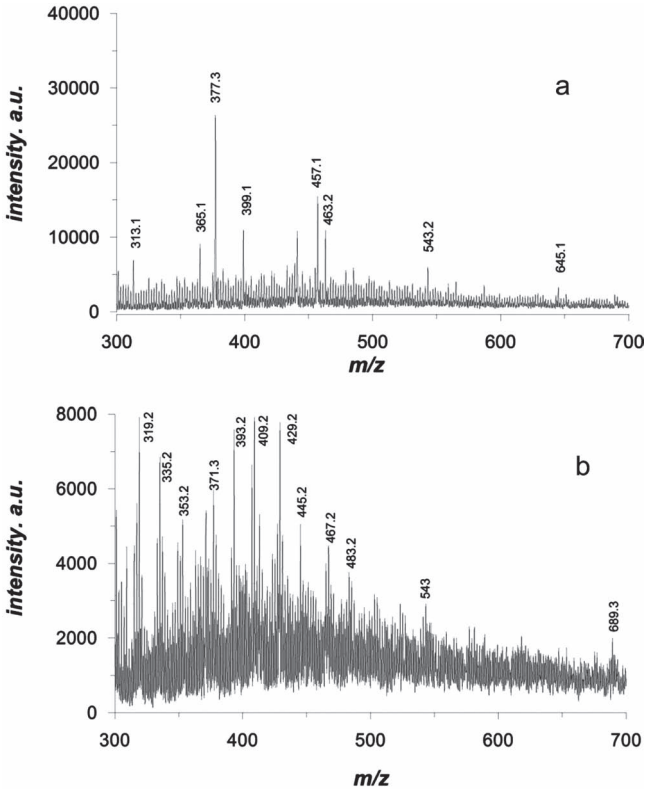

Figure 3. LDI-MS spectra of polydopamine samples 2 (panel a) and 6 (panel b) prepared from 0.5×10^{-3} M dopamine in 0.1 M phosphate buffer and 0.05 M Tris, respectively.

form mixtures of oligomer/polymer species, apparently in contrast with the recently proposed quinhydrone-type monomeric structure.[26] Since, however, the latter structure was worked out from a polydopamine sample obtained under different conditions (5×10^{-3} M Tris at uncontrolled pH), it seems that some of the conclusions of that study do not apply to the present set of polydopamine samples, and vice versa. To better clarify this point, we carried out a comparative investigation by laser desorption ionization mass spectrometry (LDI-MS) of representative polydopamine samples described in this study against a sample prepared in Tris buffer, as recently reported.[26] **Figure 3** shows the LDI spectra of samples 2 (panel a) and 6 (panel b). The complete set of spectra, including those in Figure 3, is reported in the Supporting Information, Figure S6, and a summarizing table comparing the main peaks from the various samples is given in Table S2 in the Supporting Information.

The data show that the peak patterns vary significantly from sample to sample reflecting both the buffer and the substrate concentration, though several peaks in common between different polydopamine samples were noticed (Supporting Information, Table S2). The detected peaks were all in the range from m/z = 319 to 689. Interestingly, peaks close to m/z values of 303 and 454 were detected in various polydopamine samples, suggesting a possible relationship with the proposed physical trimer.[27] The sample prepared in 5×10^{-3} M Tris[26] generated a peak pattern different from those of the other samples, with only one main peak at m/z = 393 in common with the analogous pigment produced in 50×10^{-3} M Tris buffer. A tentative assignment of the main peaks of the various pigment samples (reported in Supporting Information, Figure S7) suggested oligomer components up to the tetramer level and incorporating different combinations of intact dopamine units, cyclized DHI units, and pyrrolecarboxylic acid fragments. Partial decarboxylation is also apparent in the LDI process at 300 °C. This was confirmed by thermogravimetric analysis indicating some 10% weight loss following heating. Structural motifs incorporating Tris moieties could also be identified in the polydopamine preparations from that buffer.

2.4. UV–Visible Spectroscopy

To gain further insight into the structural changes of polydopamine with preparation conditions, the absorption spectra of the species produced by the oxidation of dopamine at two different concentrations (0.5 and 10×10^{-3} M) were recorded. The results (Supporting Information, Figure S8) showed that the oxidation products from 0.5×10^{-3} M dopamine (panel a) exhibit a modest UV band around 280 nm and a featureless absorption throughout the entire visible region associated with significant scattering, denoting a eumelanin-like character.[41] In contrast, the products obtained from 10×10^{-3} M dopamine (panel b) showed an intense and well-defined UV band around 280 nm with a relatively less-intense absorption in the visible region, indicating a different profile with respect to typical eumelanin-like chromophores.[4] These differences would support the presence of a higher proportion of DHI-related units, the key determinants of the eumelanin visible chromophore, in the samples from low (0.05×10^{-3} M) dopamine concentration. On the other hand, the intense band at 280 nm in the samples from 10×10^{-3} M dopamine would reflect the presence of significant levels of uncyclized units.

In a separate series of experiments, the effect of varying Tris concentration on the absorption properties of polydopamine obtained by aerial oxidation of 0.5×10^{-3} M dopamine was investigated. The results (Supporting Information, Figure S8c) revealed a marked increase in the overall absorption intensity with increasing buffer concentration, with a slight concomitant enhancement of the UV band around 280 nm. No detectable effect of the buffer up to 50×10^{-3} M concentration was apparent in the oxidation of 10×10^{-3} M dopamine (not shown). The observed concentration-dependent effect of Tris would apparently reflect structural modifications and a higher degree of solubility deriving from the proposed covalent conjugation of the buffer to dopamine, but this requires verification in future work.

2.5. Polydopamine Formation Pathways

Altogether, the results reported above, together with a detailed HPLC analysis (see Supporting Information and Figure S9), concurred to delineate a complex picture of polydopamine buildup which starts from the *o*-quinone, as depicted in **Scheme 2**. In this scheme, dopamine quinone, just formed, would partition between three main competing pathways. In path a, dimerization of dopamine would lead to uncyclized,

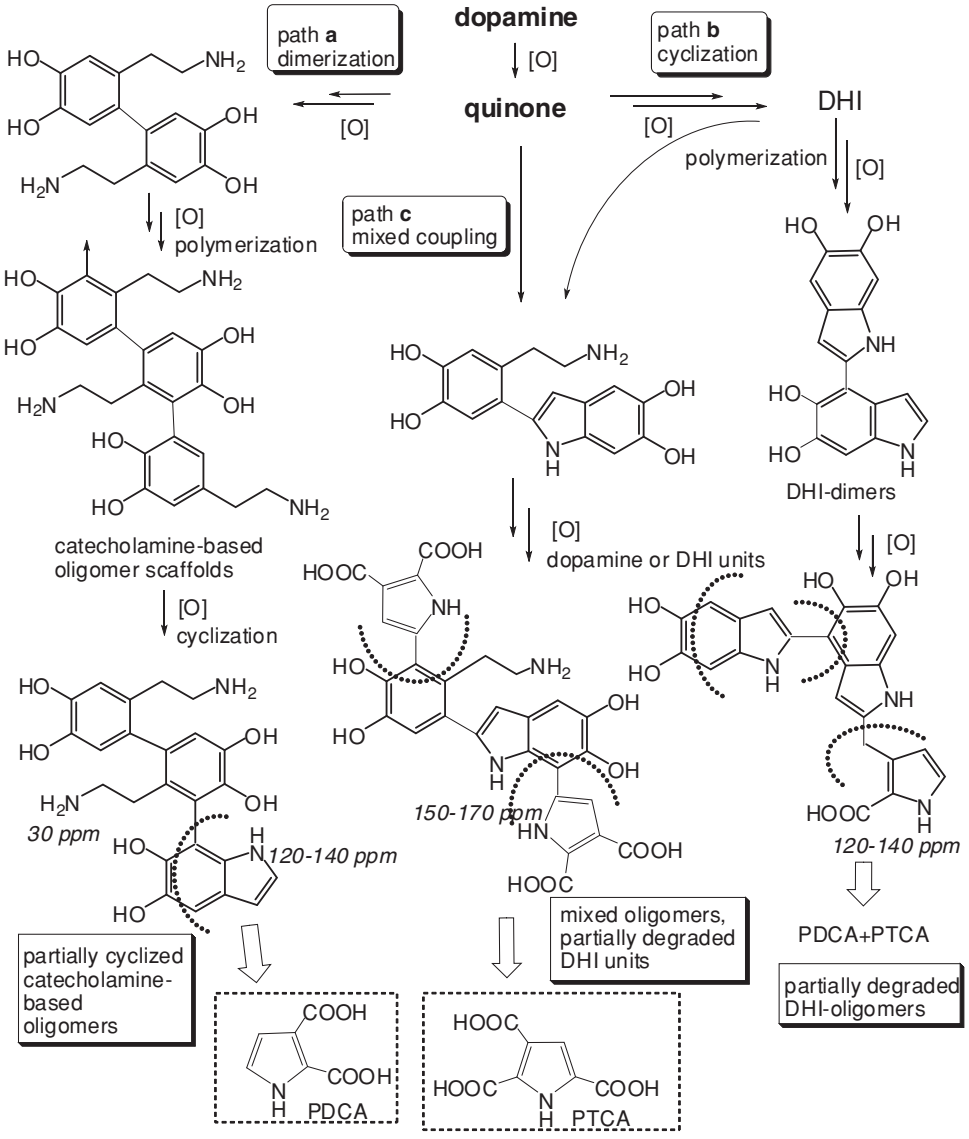

Scheme 2. Simplified overall view of main reaction pathways involved in polydopamine formation. A proposed origin of the eumelanin markers, PDCA and PTCA, is highlighted.

biphenyl-type structures. Uncyclized units would then undergo further oxidation and intramolecular cyclization, to generate DHI units unsubstituted on the 2-position.

In path b, DHI-based structures arising along typical eumelanin-forming pathways may grow and suffer partial oxidative cleavage under the autoxidative conditions of the process, due to hydrogen peroxide generation. As a result, partial peroxidative fission of *o*-quinone moieties may occur, leading to pyrrole-carboxylic acid formation.

A third route, indicated as path c, may operate at different levels following dopamine quinone formation, leading to mixed species, for example by attack of DHI to various monomer and oligomer quinone species. By the combination of these routes, an unusual, multifunctional system would result which integrates and exposes diverse groups and structural moieties, including planar indole units, catechol or quinone functions and amino and carboxylic acid groups. Little is known regarding the redox state of the structural components, although there is now solid evidence that the black color of eumelanin-type polymers reflects the presence of electron-deficient quinone moieties.[41]

The chemistry illustrated in Scheme 2, explained in more detail in the Supporting Information, integrates and expands the new concepts on the polydopamine structure presented in the latest studies.[26,27] With one of them,[27] this paper shares the conclusion that covalent-bond formation is critical during the initial steps of polydopamine buildup. Consistent with this view is the entire set of chemical and spectral data reported herein, and especially the MS data, showing the presence of low oligomer structures which may have a bearing on the recently proposed trimerization pathway by decomposition of the self-assembled non-covalent trimer.[27] On the other hand, the MS data referring to the polydopamine samples prepared under the

present conditions and those reported in the other study,[26] and the discussion on HPLC analyses in the Supporting Information section, concurred to rule out the existence of significant levels of non-covalently bound monomer intermediates (e.g., indolines), as proposed in that paper.[26] However, it is conceivable that non-covalent interactions become significant at later stages after the oligomerization reaction has proceeded significantly. The importance of aggregation phenomena in the eumelanin structure and chromophoric properties has been emphasized recently.[41]

Two important remarks concern the role of dopamine quinone as the key control point in the polymerization pathway: 1) When the quinone is generated by autoxidation in the presence of high concentrations of dopamine (e.g., 10×10^{-3} M), it may be efficiently trapped, giving mainly dimerization products. At low dopamine concentration (0.5×10^{-3} M), on the other hand, the slowly generated quinone would be less efficiently trapped by dopamine, increasing the chances for intramolecular cyclization to give DHI. 2) Dopamine quinone, due to its relatively long lifetime,[40] provides an important target for Tris, favoring an unprecedented incorporation reaction. An interesting consequence of the conjugation reaction would be the inhibition of the intramolecular cyclization reaction, whereby the coexistence in the adduct of two amine nitrogens would cause the slightly bifurcate appearance of the ^{15}N NMR amine peaks at $\delta = 30$ and 40 ppm (Supporting Information, Scheme S2).

The proposed incorporation of Tris into polydopamine provides a convincing explanation both for the observed difficulty in collecting the material after 24 h, at variance with the other samples, and for the reported influence of the buffer on the growth regime of polydopamine films during deposition.[13]

A major implication of Scheme 2 is that polydopamine incorporates a combination of diverse functional groups, especially the basic side chain amino groups, the acidic pyrrolecarboxylic functions and the indolic/catecholic π-systems, which would specifically account for its adhesion capacity. This view was supported by brief preliminary experiments in which the adhesion of polydopamine on common materials, such as cuttings of polyethylene (PE) and poly(ethylene terephthalate) (PET) bottles, was compared by visual inspection with that of the oxidation products of DHI and hydroxytyrosol, the latter resembling dopamine but lacking the amino group on the side chain, replaced by a hydroxyl function.[42] The images in Figure S10 in the Supporting Information clearly show that only dopamine can produce visible and resistant coatings on the plastic cuttings, much darker than those from DHI, whereas hydroxytyrosol-treated plastics did not exhibit visually detectable coatings despite complete substrate oxidation. Based on these simple and qualitative observations, it can be speculated that the superior adhesion properties of polydopamine stem from the peculiar coexistence of certain specific structural features, which are lacked or possessed only separately by the other polyphenolic materials.

3. Conclusions

Using an integrated chemical and spectral approach we have shown herein that polydopamine consists of three main building blocks, uncyclized catecholamine/quinones, cyclized DHI units, and so-far-unrecognized pyrrolecarboxylic acid moieties, the latter typical of eumelanin structural motifs. Increasing the dopamine concentration leads to higher proportions of uncyclized amine-containing units, whereas lower dopamine concentrations favor higher levels of cyclized indolic components, imparting a more-defined eumelanin-like character to the material. Although these results are partly in line with recent structural insights,[26,27] they clearly show that none of the previous structural models are sufficient per se to account for the polydopamine properties. Polydopamine should now be represented at best as a collection of oligomeric species in which monomer units are linked through different bonding. Because of the current lack of evidence for a true macromolecular nature of polydopamine, we suggest also that the pigment be more properly referred to as "dopamine black".[13]

The coexistence of structurally diverse components is a distinguishing characteristic of polydopamine that accounts for a unique blend of eumelanin-like and amine-containing polycatechol functionalities. These can be manipulated rationally through the proper selection of the dopamine concentration and the buffer, which are expected to act through dopamine quinone as a sensitive control point governing the final structure and properties. The observed concentration-dependent incorporation of Tris into the polymer would explain the reported effects of the buffer on the film thickness.[13] Further insight into the dopamine-Tris coupling reaction, including a more-thorough analysis of the concentration-dependent effects, will be the goal of future studies.

4. Experimental Section

Polydopamine Synthesis: Polydopamine was prepared by autoxidation of dopamine hydrochloride (151 mg, 1 mmol) dissolved in 0.1 M bicarbonate or 0.1 M phosphate buffer at pH = 8.5 or 0.05 M Tris buffer at pH = 8.5, according to Bernsmann et al.,[13] or in 0.005 M Tris buffer, according to Dreyer et al.[26] The mixture was left under vigorous stirring. After 24 h, the reaction mixture was acidified to pH = 2 with 3 M HCl and the dark pigment that separated was collected by centrifugation at 7000 rpm at 4 °C, washed 3 times with water at pH = 3 and lyophilized for 12 h. The yields of polydopamine obtained under the different reaction conditions are reported in Table S1 in the Supporting Information.

Solid-State NMR: Solid-state ^{13}C and ^{15}N CP-MAS spectra were collected at 100.5 and 40.5 MHz, respectively, on a Bruker Avance II 400 spectrometer operating at a static field of 9.4 T, equipped with a 4 mm MAS probe. Synthesized materials and reference compounds (dopamine and Tris(hydroxymethyl aminomethane) were finely ground in a mortar and packed into 4 mm zirconia rotors sealed with Kel-F caps. The spinning speeds were set at 8 and 6 kHz for the ^{13}C and ^{15}N NMR experiments, respectively.

Cross-polarization spectra were recorded using a variable spin-lock sequence (ramp CP-MAS), and a relaxation delay of 4s; a ^{1}H $\pi/2$ pulse width of 3.0 µs was employed and high-power proton decoupling was applied during acquisition. Spectra were Fourier transformed using 512 points in the time domain and a Gaussian line broadening.

For the ^{13}C spectra, the contact time was set to 2 ms and 20 000 scans were recorded for each sample. The spectra were referenced to external adamantane (CH signal at 38.48 ppm downfield of tetramethylsilane (TMS), set at 0.0 ppm).

For the ^{15}N spectra, the contact time was set to 1.2 ms and 60 000 scans were recorded. The spectra were referenced to external glycine (amine signal 32.6 ppm downfield of ammonia, set at 0.0 ppm).

LDI Mass Spectrometry: Atmospheric-pressure laser desorption mass spectrometry (AP-LDI MS) was performed on an Agilent 1100 Series MSD Ion Trap (Agilent Technologies, Palo Alto, CA, USA). The system was equipped with a nitrogen laser (337 nm, 10 Hz pulsed beam of UV light). The ion trap scanned from m/z = 50 to 4000. Each AP-LDI mass spectrum consisted of 100–150 coadded spectra collected on the whole spot surface (1–2 mm in diameter) in order to overcome the non-homogeneity of the sample on the target plate. Additional details are given in a previous paper.[43]

Different preparation procedures were used. The samples prepared as described above under polydopamine synthesis were not subjected to lyophilization but, as obtained after centrifugation, were suspended in water (1 mg mL^{-1}) and dropped directly onto the target plate and allowed to dry before analysis. In other experiments the samples as obtained after centrifugation were suspended in 1:1 water/glycerol, left under stirring for 1 h and then taken to dryness in an oven. The powders thus obtained were then suspended in water and dropped on the plate.

Chemical Degradation: Polydopamine or eumelanin samples (5 mg) were suspended in 1 M NaOH containing 1.5% H_2O_2 (1 mL) according to a previously reported procedure[44] and kept under stirring in air. After 18 h, the mixture was acidified to pH = 2 with 0.2 M HCl and analyzed by HPLC.

Analyses of PTCA and PDCA were performed on an HPLC instrument equipped with a UV–vis detector, set at 254 and 280 nm. A Synergi Hydro-RP80A column (250 × 4.60 mm, 4 μm) was used, with 1% formic acid taken to pH = 2.8 with sodium hydroxide/methanol 97:3 (v/v) as the eluent, at a flow rate of 0.7 ml min^{-1}. For analysis of the dopamine oxidation mixture, the same column was used with UV–vis detection set at 280 or 480 nm using 1% formic acid/methanol 92:8 (v/v) as the eluent, and at a flow rate of 0.7 mL min^{-1}.

All of the experiments were run in triplicate, and the HPLC analyses were run in triplicate for each experiment. The mean and standard deviations were calculated using Excel software. Differences in the PTCA and PDCA yields among the different samples were statistically analyzed by one way-analysis of variance (ANOVA) *t*-tests, and were considered significant with $p < 0.05$.

Supporting Information

Supporting Information is available from the Wiley Online Library or from the author.

Acknowledgements

This work was supported by grants from Italian MIUR, PRIN 2008 project, and was carried out within the aims of the EuMelaNet special interest group (http://www.espcr.org/eumelanet/).

Received: July 27, 2012
Revised: September 7, 2012
Published online: October 9, 2012

[1] S. Ito, K. Wakamatsu, M. d'Ischia, A. Napolitano, A. Pezzella, in *Melanins and Melanosomes: Biosynthesis, Biogenesis, Physiological, and Pathological Functions* (Eds: P. A. Riley, J. Borovansky) Wiley-VCH, Germany **2011**, *Ch. 6*, 167–185.
[2] M. d'Ischia, A. Napolitano, A. Pezzella, P. Meredith, T. Sarna, *Angew. Chem. Int. Ed. Engl.* **2009**, *48*, 3914.
[3] J. D. Simon, L. Hong, D. N. Peles, *J. Phys. Chem. B* **2008**, *112*, 13201–13217.
[4] P. Meredith, T. Sarna, *Pigment Cell Res.* **2006**, *19*, 572–594.
[5] A. Napolitano, P. Manini, M. d'Ischia, *Curr. Med. Chem.* **2011**, *18*, 1832–1845.
[6] G. Prota, M. d'Ischia, D. Mascagna, *Melanoma Res.* **1994**, *4*, 351–358.
[7] A. Napolitano, A. Pezzella, G. Prota, *Chem. Res. Toxicol.* **1999**, *12*, 1090–1097.
[8] M. d'Ischia, G. Prota, *Pigment Cell Res.* **1997**, *10*, 370–376.
[9] H. Lee, S. M. Dellatore, W. M. Miller, P. B. Messersmith, *Science* **2007**, *318*, 426–430.
[10] J. H. Waite, *Nat. Mater.* **2008**, *7*, 8–9.
[11] Q. Ye, F. Zhou, W. Liu, *Chem Soc. Rev.* **2011**, *40*, 4244–4258.
[12] B. P. Lee, P. B. Messersmith, J. N. Israelachvili, J. H. Waite, *Annu. Rev. Mater. Res.* **2011**, *41*, 99–132.
[13] F. Bernsmann, V. Ball, F. Addiego, A. Ponche, M. Michel, J. J. de Almeida Gracio, V. Toniazzo, D. Ruch, *Langmuir* **2011**, *27*, 2819–2825.
[14] J. Cui, Y. Wang, A. Postma, J. Hao, L. Hosta-Rigau, F. Caruso, *Adv. Funct. Mater.* **2010**, *20*, 1625–1631.
[15] S. H. Yang, S. M. Kang, K.-B. Lee, T. D. Chung, H. Lee, I. S. Choi, *J. Am. Chem. Soc.* **2011**, *133*, 2795–2797.
[16] J. Ryu, S. H. Ku, M. Lee, C. B. Park, *Soft Matter* **2011**, *7*, 7201–7206.
[17] M. E. Lynge, R. van der Westen, A. Postma, B. Städler, *Nanoscale* **2011**, *3*, 4916–4928.
[18] V. Ball, D. Del Frari, M. Michel, M. J. Buehler, V. Toniazzo, M. K. Singh, J. Gracio, D. Ruch, *BioNanoScience* **2012**, *2*, 16–34.
[19] M. H. Ryu, Y. M. Lee, J. K. Park, J. W. Choi. *Adv Mater.* **2011**, *19*, 3066–3070.
[20] I. You, S. M. Kang, S. Lee, Y. O. Cho, J. B. Kim, S. B. Lee, Y. S. Nam, H. Lee *Angew. Chem. Int. Ed.* **2012**, *51*, 6126–6130.
[21] S. M. Kang, I. You, W. K. Cho, H. K. Shon, T. G. Lee, I. S. Choi, J. M. Karp, H. Lee *Angew. Chem. Int. Ed.* **2010**, *49*, 9401–9404.
[22] B. Yu, J. Liu, S. Liu, F. Zhou, *Chem. Commun.* **2010**,*46*, 5900–5902.
[23] O. Crescenzi, C. Kroesche, W. Hoffbauer, M. Jansen, A. Napolitano, G. Prota, M. G. Peter, *Liebigs Ann. Chem.* **1994**, *6*, 563–567.
[24] K.-Y. Ju, Y. Lee, S. Lee, S. B. Park, J.-K. Lee, *Biomacromolecules* **2011**, *12*, 625–632.
[25] J.-H. Jiang, L.-P. Zhu, X.-L. Li, Y.-Y. Xu, B.-K. Zhu, *J. Membr. Sci.* **2010**, *364*, 194–202.
[26] D. R. Dreyer, D. J. Miller, B. D. Freeman, D. R. Paul, C. W. Bielawski, *Langmuir* **2012**, *28*, 6428–6435.
[27] S. Hong, Y. S. Na, S. Choi, I. T. Song, W. Y. Kim, H. Lee, *Adv. Funct. Mater.* **2012**, DOI: 10.1002/adfm.201201156.
[28] M. d'Ischia, A. Napolitano, A. Pezzella, *Eur. J. Org. Chem.* **2011**, 5501–5516.
[29] M. d'Ischia, A. Napolitano, A. Pezzella, E. J. Land, C. A. Ramsden, P. A. Riley, *Adv. Heterocycl. Chem.* **2005**, *89*, 1–63.
[30] A. Pezzella, L. Panzella, O. Crescenzi, A. Napolitano, S. Navaratman, R. Edge, E. J. Land, V. Barone, M. d'Ischia, *J. Am. Chem. Soc.* **2006**, *128*, 15490–15498.
[31] A. Pezzella, L. Panzella, A. Natangelo, M. Arzillo, A. Napolitano, M. d'Ischia, *J. Org. Chem.* **2007**, *72*, 9225–9230.
[32] A. Napolitano, A. Palumbo, M. d'Ischia, G. Prota, *J. Med. Chem.* **1996**, *39*, 5192–5201.
[33] M. Arzillo, A. Pezzella, O. Crescenzi, A. Napolitano, E. J. Land, V. Barone, M. d'Ischia, *Org. Lett.* **2010**, *12*, 3250–3253.
[34] L. Panzella, A. Pezzella, A. Napolitano, M. d'Ischia, *Org. Lett.* **2007**, *9*, 1411–1414.
[35] A. Napolitano, A. Pezzella, M. d'Ischia, G. Prota, *Tetrahedron* **1996**, *52*, 8775–8780.
[36] K. Wakamatsu, S. Ito, *Pigment Cell Res.* **2002**, *15*, 174–183.
[37] A. Napolitano, A. Pezzella, M. R. Vincensi, G. Prota, *Tetrahedron* **1995**, *51*, 5913–5920.
[38] B. B. Adhyaru, N. G. Akhmedov, A. R. Katritzky, C. R. Bowers, *Magn. Reson. Chem.* **2003**, *41*, 466–474.

[39] A. B. Patel, E. Crocker, P. J. Reeves, E. V. Getmanova, M. Eilers, H. G. Khorana, S. O. Smith, *J. Mol. Biol.* **2005**, *347*, 803–812
[40] S. Ito, *Pigment Cell Res.* **2003**, *16*, 230–236.
[41] A. Pezzella, A. Iadonisi, S. Valerio, L. Panzella, A. Napolitano, M. Adinolfi, M. d'Ischia, *J. Am. Chem. Soc.* **2009**, *131*, 15270–15275.
[42] M. De Lucia, L. Panzella, A. Pezzella, A. Napolitano, M. d'Ischia, *Tetrahedron* **2006**, *62*, 1273–1278.
[43] M. Alfè, B. Apicella, A. Tregrossi, A. Ciajolo, *Carbon* **2008**, *46*, 2059–2066.
[44] L. Panzella, P. Manini, G. Monfrecola, M. d'Ischia, A. Napolitano, *Pigment Cell Res.* **2007**, *20*, 128–133.